Evaluation of Aerosol Chemical Composition Simulations by the WRF-Chem Model at the Puy de Dôme Station (France)

Christelle Barbet, Laurent Deguillaume, Nadine Chaumerliac, Maud Leriche, Evelyn Freney, Aurélie Colomb, Karine Sellegri, Luc Patryl, Patrick Armand

Aerosol and Air Quality Research, 16: 909–917, 2016

ISSN: 1680-8584 print / 2071-1409 online
doi: 10.4209/aaqr.2015.05.0342

Evaluation of Aerosol Chemical Composition Simulations by the WRF-Chem Model at the Puy de Dôme Station (France)

Christelle Barbet[1,2], Laurent Deguillaume[1,2], Nadine Chaumerliac[1,2*], Maud Leriche[3,4], Evelyn Freney[1,2], Aurélie Colomb[1,2], Karine Sellegri[1,2], Luc Patryl[5], Patrick Armand[5]

[1] *Université Clermont Auvergne, Université Blaise Pascal, OPGC, Laboratoire de Météorologie Physique, 4 av. Blaise Pascal TSA 60026 CS 60026 63178 Aubière Cedex, France*
[2] *CNRS, LaMP/OPGC, UMR6016, 4 av. Blaise Pascal TSA 60026 CS 60026 63178 Aubière Cedex, France*
[3] *Université de Toulouse, UPS, Laboratoire d'Aérologie, 14 avenue Edouard Belin, 31400 Toulouse, France*
[4] *CNRS, LA, UMR5560, 31400 Toulouse, France*
[5] *CEA, DAM, DIF, F-91297 Arpajon, France*

ABSTRACT

The high altitude Puy de Dôme (PUY) research station, located at 1465 m a.s.l. in central France, hosts many instruments allowing continuous measurements and intensive campaigns to measure meteorological parameters, gas-phase species, aerosol and cloud properties. Aerosol chemical composition measurements provided by a compact Time-of-Flight Aerosol Mass Spectrometer (cToF-AMS) are used to evaluate the WRF-Chem model and more precisely its ability to simulate organic aerosol (OA) for a particular event in summer 2010. Using the Volatility Basis Set approach (VBS), dedicated to the formation of secondary organic aerosol (SOA), the WRF-Chem model strongly underestimates the high concentration levels of OA observed at the PUY station: 12.5 μg m^{-3} were observed and only 2.6 μg m^{-3} were simulated. By means of several measurements of gas-phase volatile organic compounds (VOCs), the robustness of both emissions and SOA formation processes in the WRF-Chem model was tested. The underestimation of the OA mass concentration appears to be mainly due to a misrepresentation of the oxidation rate of the organic condensable vapours (OCVs) and the SOA yields of both anthropogenic and biogenic VOCs in the VBS parameterization.

Keywords: Organic aerosol; Chemistry/Transport model; Emission inventory; Secondary Organic Aerosol (SOA) formation.

INTRODUCTION

In the atmosphere, aerosol particles have major impacts on climate, air quality and human health (IPCC, 2013). Organic aerosol (OA) represents 20 to 90% of the submicron particulate mass (Zhang *et al.*, 2007) dependent on location, season and long-range transport conditions. OA is traditionally divided into two categories: primary organic aerosol (POA) directly emitted into the atmosphere and secondary organic aerosol (SOA) produced through a gas-to-particle conversion involving Volatile Organic Compounds (VOCs) with their various volatilities. SOA represents the predominant fraction of OA (from 63 to 95%; Zhang *et al.*, 2011). Despite the abundance of OA in the atmosphere, there are still large uncertainties in understanding their formation pathways (Hallquist *et al.*, 2009).

Fields measurements indicate that the gaseous precursors and the primary particles emitted by biogenic sources are the main sources of OA over the European continent in summer (Gelencsér *et al.*, 2007). Analysis of OA mass spectra provided by an Aerosol Mass Spectrometer (AMS) demonstrate that the contribution of oxygenated organic aerosol (OOA), produced through gas to particle conversion, is predominant during summer (Lanz *et al.*, 2010). Some aircraft and ground-based measurements showed that the OA contribution to the total particulate matter is lower in the boundary layer than in the free troposphere (Crumeyrolle *et al.*, 2013). According to the air masses transport pathways, the mass concentrations of the OA vary: the highest concentrations are measured for air masses transported over polluted areas (Freutel *et al.*, 2013). To interpret such observations and describe the OA variations, chemistry-transport models are appropriate tools as they allow studying simultaneously the emissions, the transport and the physical-chemical transformations of gas phase species and aerosol particles. However, whatever scale is considered (regional or global), large gaps still remain between modelled and measured SOA concentrations and more particularly for

* Corresponding author.
Tel.: (+33) 04 73 40 73 72; Fax: (+33) 04 73 40 51 36
E-mail address: n.chaumerliac@opgc.univ-bpclermont.fr

summer periods (Knote *et al.*, 2011). The underestimation of the organic aerosol concentrations is observed in most modelling studies (de Gouw, 2005; Heald *et al.*, 2005; Jimenez *et al.*, 2009; Hodzic *et al.*, 2010; Yu, 2011). Several recent regional modeling studies are accounting for the semi-volatile nature and chemical aging of organic compounds both in the gas phase (OCVs which are the first generation VOC oxidation products) and/or in the aerosol phase demonstrating improvements in reproducing the organic aerosol budget and its chemical resolution (Murphy and Pandis, 2009; Tsimpidi *et al.*, 2010; Shrivastava *et al.*, 2011; Ahmadov *et al.*, 2012; Bergström *et al.*, 2012; Athanasopoulou *et al.*, 2013; Zhang *et al.*, 2013; Fountoukis *et al.*, 2014). Langmann *et al.* (2014) found that the OA mass concentrations are in the range of the measurements performed at the Puy de Dôme station by increasing the BVOCs emissions by a factor of 5 and considering that 10% of the secondary organic compounds reach a saturation vapour pressure low enough to move into the next lower volatility category.

In this paper, the Weather Research and Forecasting – Chemistry model (WRF-Chem; Grell *et al.*, 2005) and the 1D-Volatity Basis Set (1D-VBS; Donahue *et al.*, 2006) approach dedicated to the SOA formation and aging are used to re-evaluate measurements performed at the Puy de Dôme for the same 2010 summer period as Langmann *et al.* (2014). Moreover, in this study, measurements of the gaseous precursors (anthropogenic and biogenic VOCs) of SOA are available to complement AMS measurements and allow testing the uncertain parameters involved in the SOA formation in the WRF-Chem model such as emissions and SOA formation processes.

METHODS

WRF-Chem Model Configuration

The version 3.4.1 of the online WRF-Chem model (http://ruc.noaa.gov/wrf/WG11/) is used in this study. The main physical and chemical parameterizations adopted in the WRF-Chem model for this study are listed in Table 1. The simulations, which last one week, are performed over two nested domains: a coarse domain located over Europe and an inner domain located over France, with spatial resolutions of 30 km and 10 km respectively. To better represent the lower layers of the atmosphere and the variations of the boundary layer height, an enhanced resolution in the lower atmosphere is used for vertical levels.

The initial and boundary meteorological conditions (Dee *et al.*, 2011) are provided by the European Centre for Medium-range Weather Forecast (ECMWF) with a temporal resolution of 6 hours and a horizontal resolution of 0.5°. The initial and boundary conditions for gaseous species and aerosol particles concentrations come from the global model MOZART-4 (Emmons *et al.*, 2010). They are available every 6 hours with a horizontal resolution in latitude and longitude of 1.9° per 2.5°.

Anthropogenic emissions are derived from the MACCity inventory (MACC/CityZEN EU projects; Granier *et al.*, 2011). MACCity provides emission fluxes for gaseous (CO, SO_2, NH_3, NO_x, VOCs) and aerosol (organic carbon (OC) and elemental carbon (EC)) species with a monthly temporal resolution and a spatial resolution of 0.5° per 0.5°. The VOCs emissions are disaggregated into the Regional Atmospheric Chemistry Mechanism (RACM; Stockwell *et al.*, 1997; Geiger *et al.*, 2003) model species following the aggregation procedure proposed by Middleton *et al.* (1990). To convert the emissions of OC into POA, a conversion factor of 1.6 is used as proposed by Bessagnet *et al.* (2008). Then, 20% and 80% of POA and EC are allocated respectively to the Aïtken and the accumulation modes of the aerosol lognormal distribution (Ackermann *et al.*, 1998).

Biogenic emissions are calculated online using the Model of Emissions of Gases and Aerosol from Nature (MEGAN; Guenther *et al.*, 2006) that uses a 1 × 1 km resolution to quantify the net emissions of isoprene and estimate the emissions of monoterpenes, oxygenated compounds, sesquiterpenes and nitrogen oxide.

Biomass burning emissions are derived from the Fire Inventory from NCAR version 1.0 (FINNv1; Wiedinmyer *et al.*, 2011) that provides global estimates of gas (CO_2, CO, CH_4, VOCs, H_2, NO_x, NH_3, SO_2) and aerosol particles (OC, BC, $PM_{2.5}$, PM_{10}) emissions with a daily temporal resolution and a spatial resolution close to 1 km.

Measurements

The PUY research station, located in the middle of France (45.46°N, 2.57°E) at 1465 m a.s.l, is part of the Aerosols, Clouds, and Trace gases Research InfraStructure (ACTRIS) and Global Atmosphere Watch (GAW) networks. This station is equipped with a wide range of instruments providing information on meteorological parameters, gas-phase species concentrations and aerosol properties. It also hosts intensive

Table 1. WRF-Chem configuration.

Process	WRF-Chem option	
Land-surface model	Noah Land Surface Model	(Chen and Dudhia, 2001)
Boundary layer scheme	Yonsei University	(Hong *et al.*, 2006)
Long-wave radiation	Rapid Radiation Transfer Model	(Mlawer *et al.*, 1997)
Short-wave radiation	Goddard	(Chou *et al.*, 1998)
Microphysics	Morrison	(Morrison *et al.*, 2009)
Cumulus parameterization	Grell-Devenyi	(Grell and Dévényi, 2002)
Gas-phase mechanism parameterization	RACM	(Stockwell *et al.*, 1997)
Aerosol parameterization	MADE/ VBS	(Ackermann *et al.*, 1998) (Ahmadov *et al.*, 2012)

measurements campaigns during which further instruments are deployed at the station. Among them, the cToF-AMS (Canagaratna *et al.*, 2007) provides detailed information on the chemical composition and mass concentration of the non-refractory submicron particulate matter (NR-PM_1). VOCs species measurements performed by gas chromatography-mass spectrometry (GC/MS), which is an analytical technique that combines the performance of gas chromatography, for separating compounds of a sample, and mass spectrometry for the detection and identification of compounds based on their mass/load ratio, are also available at the PUY station since 2010.

As part of a EMEP intensive measurements campaign, detailed investigations were performed at the PUY station to characterize chemical and microphysical aerosol properties for several periods by Freney *et al.* (2011). In this paper, the summer 2010 case (from the 23rd to the 27th of June 2010) has been selected because it is the longest event with very high levels in aerosol concentrations within the same polluted continental air mass.

RESULTS AND DISCUSSION

Boundary Layer Height and Volatile Organic Compounds Concentrations

A recent study, based upon LIDAR measurements follows the seasonal variations of the boundary layer height (BLH) at the PUY station (Hervo *et al.*, 2014). This study shows that the summit is mainly located in the free troposphere during winter and at night-time while in daytime summer it is merged into the boundary layer (BL). Further comparisons between the BLH retrieved from LIDAR profiles and the time series of BL tracers were conducted in Rose *et al.* (2014), indicating that there were little forced convection effects from the PUY on the BL dynamics, likely due to its relatively isolated peak topographic configuration.

WRF-Chem model is able to reproduce the general diurnal evolution of the BLH observed by Hervo *et al.* (2014) (red line in Fig. 1). At the Puy de Dôme the surface elevation calculated by the model is 799 m (dotted black line in Fig. 1) instead of 1465 m (the real altitude of the Puy de Dôme (black line in Fig. 1)). This is due to the resolution of the topography in the model. For this reason, according to the model, the summit would be always located in the BL independently of the season. Instead of discussing the results for the modeled altitude of the Puy de Dôme, results are discussed for the real altitude of the station, at 1465 m. It is worth mentioning that at 1465 m, meteorological parameters such as temperature and humidity reflect best the measurements performed at the station (Fig. S1).

During the 2010 campaign, three biogenic VOCs (BVOCs) were measured at the PUY station: α-pinene, β-pinene and limonene. In the model, "API" species groups together α-pinene with β-pinene and other cyclic terpenes with one double bond, and "LIM" species groups together limonene with d-limonene and other cyclic diene-terpenes. After their oxidation, these BVOCs can contribute to the formation of SOA. Their SOA yields range from 20% to 60% according to their initial concentrations, the NO_x concentrations, the type of oxidants, the temperature, the relative humidity and the radiation.

Simultaneously, several anthropogenic VOCs (AVOCs) were measured: n-octane and n-nonane, benzene, toluene and ethylbenzene and o-; m-; p-xylenes, 2-; 3-; 4-ethyltoluene and 1,2,4-; 1,2,3- and 1,3,5-trimethylbenzene. As these AVOCs are not represented individually in the model, they are lumped in the model species. Thus, the "HC8" species in the model groups together n-octane and n-nonane, the "TOL" species groups benzene, toluene and ethylbenzene and the "XYL" species groups o-; m-; p-xylenes, 2-; 3-; 4-ethyltoluene and 1,2,4-; 1,2,3- and 1,3,5-trimethylbenzene.

Fig. 1 shows the temporal evolution of BVOCs and AVOCs simulated and observed but also the variations of the BLH simulated by the WRF-Chem model. Despite an underestimation of the concentration levels (by factors 2 and 10 respectively for pinenes and limonene), the model well captures the diurnal variation of pinene (Fig. 1(A)) and limonene (Fig. 1(B)) with lower concentrations levels during nighttime, when the PUY station is located in the free troposphere, than during daytime, when the PUY station is located in the boundary layer. For the AVOCs (alkanes: Fig. 1(C), xylene: Fig. 1(D) and toluene: Fig. 1(E)), the underestimation of the concentration levels is strongest than for BVOCs. The evolution of the concentrations of AVOCs seems to be correlated with the time evolution of the BLH. Indeed, the concentrations of these species increase as soon as the Puy de Dôme enters in the boundary layer and then decrease when the summit leaves the boundary layer.

Aerosol Particles

The time evolutions of sulphate (SO_4^{2-}), nitrate (NO_3^-), ammonium (NH_4^+), chloride (Cl^-), black carbon (BC) and organics mass concentrations measured at the PUY station and simulated by the WRF-Chem model are presented in Fig. 2. The average mass concentration observed (21.3 μg m^{-3}) in summer 2010 is strongly underestimated by the model (7.5 μg m^{-3}). At the PUY station (Fig. 2(a)), the average organic species mass concentrations measured represent 11.2 μg m^{-3}, sulphates 3.2 μg m^{-3}, ammonium 2.4 μg m^{-3}, nitrates 1.8 μg m^{-3}, black carbon 0.4 μg m^{-3} and chloride particles 0.06 μg m^{-3}. In the WRF-Chem model (Fig. 2(b)), organic species represent on average 2.0 μg m^{-3}, sulphates 3.0 μg m^{-3}, ammonium 1.4 μg m^{-3}, nitrates 0.9 μg m^{-3} and black carbon 0.2 μg m^{-3}.

There is some model underestimation for nitrate and ammonium, probably due to some residual sources caused by agricultural activities that are not well considered in the model. Analysis of aerosol chemistry measurements in a number of stations all over Europe has shown that organic nitrates can represent 34% to 44% of the measured aerosol nitrate and are found at all urban and rural sites (Kiendler-Scharr *et al.*, 2015). This significant contribution to particulate nitrate is not considered in the model and could explain why nitrate is underestimated.

The highest underestimation appears for the mass concentration of OA, which is 6 times lower in the model than in the observations. Using the available measurements, a series of sensitivity tests have been performed to attempt to

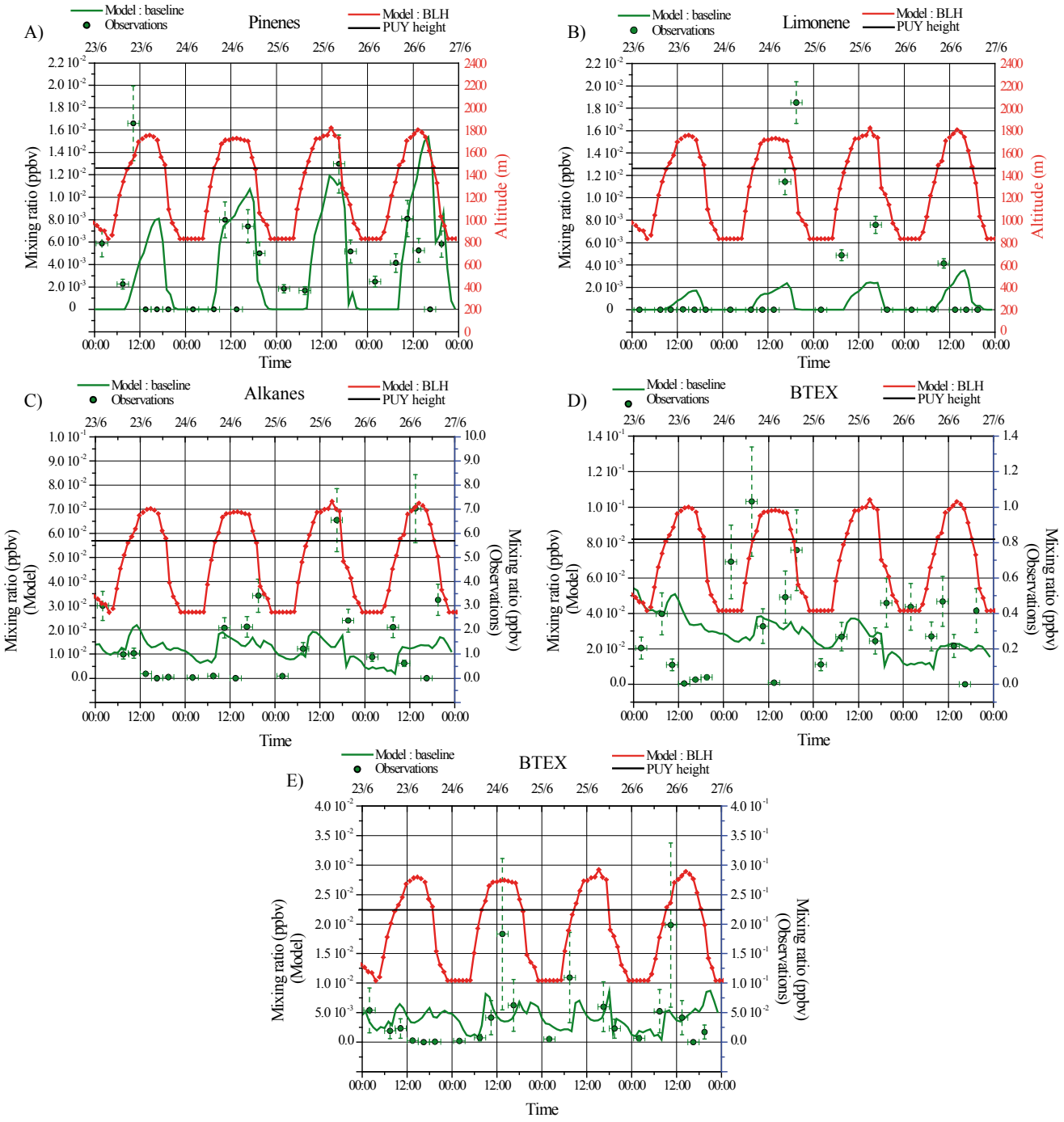

Fig. 1. VOCs mixing ratios measured at the PUY station and simulated by the WRF-Chem for the baseline simulation and boundary layer height (BLH in red) simulated by the WRF-Chem model. The red plots used for BL height are similar for all figures. BL height scale is indicated in Figs. 1(A)/1(B) on the right and is not reported in Figs. 1(C)/1(D)/1(E) for clarity. A) [α-pinene + β-pinene] vs. [API model species]; B) [limonene] vs. [LIM model species]; C) [n-octane + n-nonane] vs. [HC8 model species]; D) [benzene, toluene + ethylbenzene] vs. [TOL model species] and E) [o-; m-; p-xylenes, 2-; 3-; 4-ethyltoluene + 1,2,4-; 1,2,3-; 1,3,5-trimethylbenzene] vs. [XYL model species].

explain the differences between the OA mass concentrations simulated and observed.

Sensitivity Tests on Parameters Controlling OA Formation and Evolution

Several parameters are sources of uncertainties in the representation of OA formation in the model: emissions of gas-phase precursors of SOA but also parameters such as SOA yields and oxidation rates of OCVs that control the SOA formation.

As already mentioned, the model underestimates the concentrations of BVOCs observed by at least a factor 2.

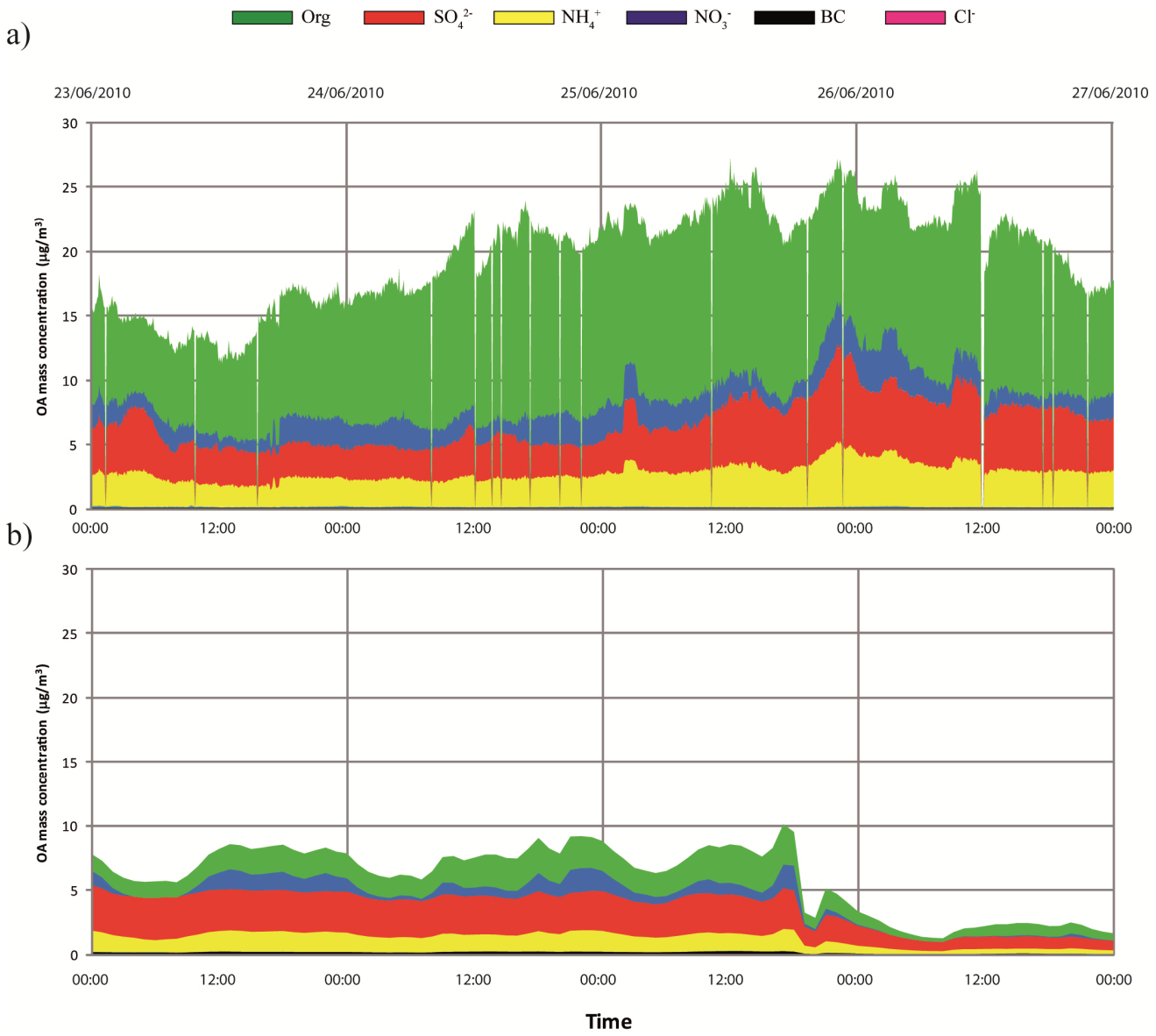

Fig. 2. Temporal evolution of the aerosol mass concentrations (µg m^{-3}) measured at the PUY station (a) and simulated by the WRF-Chem model for the baseline simulation (b).

The first test consists of doubling the BVOCs emissions that leads, as shown in Table 2, to an increase of the OA mass concentration by 18% (from 2.0 µg m^{-3} for the baseline simulation to 2.4 µg m^{-3} for the sensitivity test). The comparisons between AVOCs measured and simulation results highlighted a strong underestimation of HC8, TOL and XYL species by the model. As observations are not available for the others AVOCs, it is difficult to determinate an accurate correction factor. So, the emissions of the AVOCs have been increased by a factor of 2, as has been done for the BVOCs emissions. The average OA mass concentration slightly increases by doubling the amount of AVOCs emissions: from 2.0 to 2.5 µg m^{-3} (+ 25%). So, the impact of increasing the AVOCs emissions is equivalent to the one of increasing the BVOCs emissions.

In the model, the SOA yields defined in the VBS parameterization (Ahmadov *et al.*, 2012) and the oxidation rate of OCVs by $HO^{\bullet}$ are the two main parameters that drive the OA formation. The SOA yields, i.e., the mass of SOA produced per mass of reacted precursor, depend on both the organic precursor molecules and on the oxidants initiating the degradation. SOA yields in the model (Table S1) are based on smog chamber studies (Murphy and Pandis, 2009), where several single VOCs are oxidized under specific conditions (temperature, relative humidity, NO_x concentrations, …). The individual yields of each VOC are summed to model SOA from multiple species. However, due to the myriad of VOCs present in the atmosphere, it is not realistic to provide SOA yields for all these species through experimental studies and the extrapolation of chamber-derived SOA yields to atmospheric conditions is an important source of error (Hao *et al.*, 2011). Specifically, Zhang *et al.* (2014) demonstrated that vapor wall loss could lead to an underestimation of SOA yields by as much as a factor of 4. Due to these potential

Table 2. OA mass concentration measured at the PUY station and modeled by the WRF-Chem model for the baseline simulation and sensitivity tests: emissions, SOA yields of VOCs/oxidation rate of OCVs and all effects. Percentages indicate the OA mass increase between baseline and test simulations.

	OA mass concentration ($\mu g\ m^{-3}$)		OA mass concentration ($\mu g\ m^{-3}$)	Variation from baseline to test simulation (%)
Observations	11.2			
Model: baseline	2.02			
Model: emissions	2.78	Emissions of AVOCs	2.54	+ 26%
		Emissions of BVOCs	2.39	+ 18%
Model: yields and oxydation rate of OCVs	8.62	Yields of AVOCs	3.27	+ 62%
		Yields of BVOCs	2.85	+ 41%
		Oxidation rate of anthropogenic OCVs	2.58	+ 28%
		Oxidation rate of biogenic OCVs	2.61	+ 29%
Model: all effects	10.10			

underestimations on the SOA yields and in order to favour SOA formation, the yields of both AVOCs and BVOCs are increased by a factor 2 (however, yields values are at most equal to 100%). When doubling the SOA yields of AVOCs, the OA mass concentration is increased from 2.0 to 3.3 $\mu g\ m^{-3}$ (+ 62%) while it is only increased from 2.0 to 2.8 $\mu g\ m^{-3}$ (+ 41%) by modifying the SOA yields of BVOCs (Table 2).

In the WRF-Chem model, to implement the oxidation reaction between OCVs and the hydroxyl radical $HO^{\bullet}$, an oxidation rate of 1.0×10^{-11} cm^3 $molecule^{-1}$ s^{-1} is used (Ahmadov *et al.*, 2012). However, the most widely used oxidation rate with the VBS approach is 4.0×10^{-11} cm^3 $molecule^{-1}$ s^{-1} (Bergström *et al.*, 2012). Applying this last oxidation rate in the WRF-Chem model to anthropogenic and biogenic OCVs improves the results: the OA mass concentration is increased by around 30% (from 2.0 to 2.6 $\mu g\ m^{-3}$) in both cases (Table 2).

Thus, the SOA yields of the VOCs and the oxidation rate of the OCVs are very sensitive parameters that drive the transfer of the VOCs from the gas to the particulate phase.

To look into more details, Fig. 3 shows the time evolution of OA mass concentrations over the time period where VOCs measurements were available. This plot can be directly compared to the results obtained by Langmann *et al.* (2014) with their regional REMOTE model. Precipitation was not measured in the Puy de Dôme after 23 June 2010, whereas models determine amount of precipitation on 26 June for the WRF-Chem model and for 24 and 28/29 June for REMOTE model. Similar to the study of Langmann *et al.* (2014), a reduction of modelled OA mass concentration is observed after June 26th in connection with a convective precipitation event. Underestimation of OA mass concentration in the model is probably due to fast convective transport that washed away chemical compounds. Both studies come to the same conclusions underlining the importance of aging processes in the formation of OA even if very different approaches for SOA formation (mixed thermodynamic-kinetic approach vs. 1D-VBS approach) are used in REMOTE and WRF-Chem model respectively. They also show that emission data on SOA precursors are missing in inventories. However, we did not increase the biogenic emissions as much as in Langmann *et al.* (2014), since we use a factor 2 increase instead of 5 and apply it to both biogenic and anthropogenic precursors of SOA. In our case, measured anthropogenic precursors were much more underestimated by the model than the biogenic ones. Only a factor of 2 difference was observed for pinenes between measurements and model results. Also, WRF-Chem model is able to reproduce the observed diurnal cycle for OA mass concentrations while this was not clearly reproduced by Langmann *et al.* (2014) with their global model. This brings two remarks, first the tests on oxidation rates of OCVs mainly by OH radical seem to stress contrasts between night and day, then using a finer resolution model allows for better comparisons with observations.

CONCLUSIONS

This paper presents a comparison between AMS measurements performed at the PUY station and WRF-Chem model outputs for a one week period in summer 2010. During this period, several measurements of VOC precursors of SOA were available allowing us to examine the sources of the measured SOA (anthropogenic vs. biogenic ones) and provided us with a good opportunity to target individual parameters implicated in the SOA formation and aging with a 10 km model resolution. The differences between modeled and measured OA mass concentrations are less important when adjusting the VOCs emissions in the model with some available measurements of VOCs. The model underestimates the unexpected high OA concentration levels observed (11.1 $\mu g\ m^{-3}$) and the VOCs concentrations are much below those observed, especially for AVOCs such as alkanes and aromatic compounds. The model underestimation appears to be mainly due to a lack in SOA formation processes. Indeed, the OA mass concentration increases by 6.6 $\mu g\ m^{-3}$ by doubling the SOA yields of both anthropogenic and biogenic VOCs and by modifying the traditional oxidation rate of OCVs from 1.0×10^{-11} to 4.0×10^{-11} cm^3 $molecule^{-1}$ s^{-1} whereas an increase of only 0.8 $\mu g\ m^{-3}$ is noticed by doubling VOCs emissions. So, the SOA yields and aging processes of OCVs are highly important in the SOA formation as already noticed by Langmann *et al.* (2014) for the same set of observations in

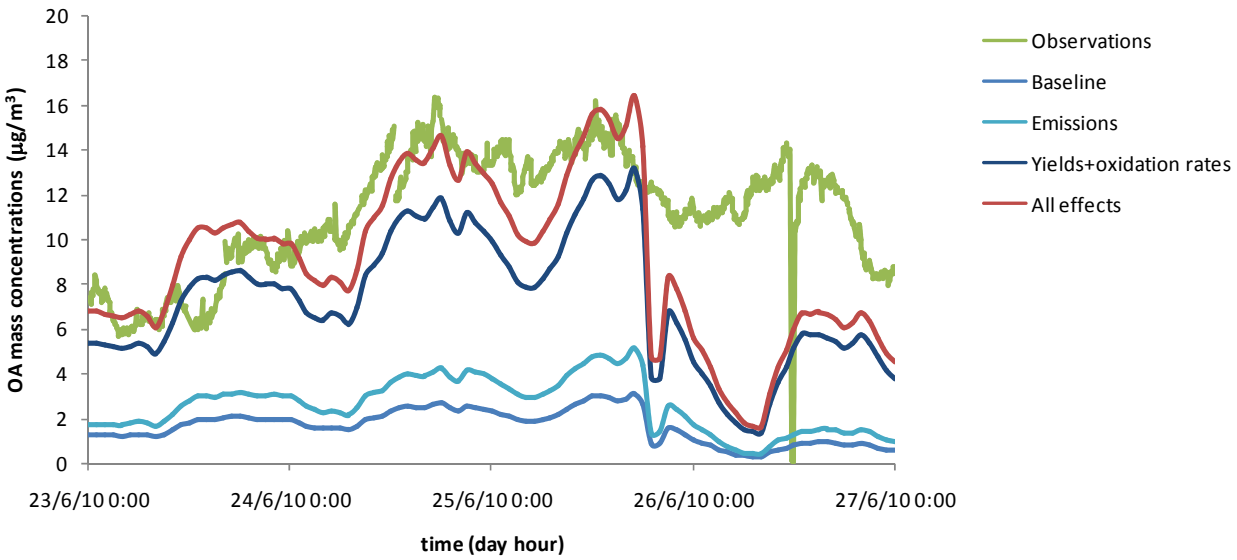

Fig. 3. Time evolution of OA mass concentration observed (in green) and simulated by the WRF-Chem model at the PUY for the baseline simulation (in red) and for sensitivity tests (with blue lines): test modifying the emissions, the SOA yields of VOCs/oxidation rate of OCVs and test with all effects cumulated.

June 2010 at the Puy de Dôme. Contrary to these authors, WRF-Chem model with a higher resolution (10 km instead of 55 km) was able to reproduce the observed diurnal cycle of OA. More VOCs and OA concentrations measurements in altitude sites are needed to improve simulations of gases and aerosols in the boundary layer and in the free troposphere.

ACKNOWLEDGMENTS

Computer resources were provided by GENCI (Grand Equipement National de Calcul Intensif) project N° 90187. The authors are very grateful to the Agence Nationale de la Recherche (ANR) for its financial support through the CUMULUS project (ANR-10-BLAN-0617). Measurements were performed within the frame of the project LEFE ATMOCHEM - Secondary organic aerosol production in the lower free troposphere over Western Europe funded by the German and French Science Foundations DFG and CNRS, and partly by the European Union FP6 Integrated project EUCAARI, contract N°.36833, 7th Framework Programme (FP7/2007-2013) within ACTRIS under grant agreement n◦ 262254 and EUSAAR (R113-CT-2006-026140). The preprocessing of emissions for the WRF-Chem model has been realized thanks to Jean-Christophe Raut, Jennie Thomas and Boris Quennehen (LATMOS: Laboratoire Atmosphères, Milieux, Observations Spatiales).

SUPPLEMENTARY MATERIALS

Supplementary data associated with this article can be found in the online version at http://www.aaqr.org.

REFERENCES

Ackermann, I.J., Hass, H., Memmesheimer, M., Ebel, A., Binkowski, F.S. and Shankar, U. (1998). Modal Aerosol Dynamics Model for Europe: Development and First Applications. *Atmos. Environ.* 32: 2981–2999, doi: 10.1016/S1352-2310(98)00006-5.

Ahmadov, R., McKeen, S.A., Robinson, A.L., Bahreini, R., Middlebrook, A.M., de Gouw, J.A., Meagher, J., Hsie, E.Y., Edgerton, E., Shaw, S. and Trainer, M. (2012). A Volatility Basis Set Model for Summertime Secondary Organic Aerosols over the Eastern United States in 2006. *J. Geophys. Res.* 117: D06301, doi: 10.1029/2011JD016831.

Athanasopoulou, E., Vogel, H., Vogel, B., Tsimpidi, A. P., Pandis, S.N., Knote, C. and Fountoukis, C. (2013). Modeling the Meteorological and Chemical Effects of Secondary Organic Aerosols during an EUCAARI Campaign. *Atmos. Chem. Phys.* 13: 625–645, doi: 10.5194/acp-13-625-2013, 2013.

Bergström, R., Denier van der Gon, H.A.C., Prévôt, A.S.H., Yttri, K.E. and Simpson, D. (2012). Modelling of Organic Aerosols over Europe (2002–2007) Using a Volatility Basis Set (VBS) Framework: Application of Different Assumptions Regarding the Formation of Secondary Organic Aerosol. *Atmos. Chem. Phys.* 12: 8499–8527, doi: 10.5194/acp-12-8499-2012.

Bessagnet, B., Menut, L., Curci, G., Hodzic, A., Guillaume, B., Liousse, C., Moukhtar, S., Pun, B., Seigneur, C. and Schulz, M. (2008). Regional Modeling of Carbonaceous Aerosols over Europe - Focus on Secondary Organic Aerosols. *J. Atmos. Chem.* 6: 175–202, doi: 10.1007/s10874-009-9129-2, 2008.

Canagaratna, M.R., Jayne, J.T., Jimenez, J.L., Allan, J.D., Alfarra, M.R., Zhang, Q., Onasch, T.B., Drewnick, F., Coe, H., Middlebrook, A., Delia, A., Williams, L.R., Trimborn, A.M., Northway, M.J., DeCarlo, P.F., Kolb, C.E., Davidovits, P. and Worsnop, D.R. (2007). Chemical and Microphysical Characterization of Ambient Aerosols with the Aerodyne Aerosol Mass Spectrometer. *Mass Spectrom. Rev.* 26: 185–222, doi: 10.1002/mas.20115.

Chen, F. and Dudhia, J. (2001). Coupling an Advanced Land Surface-hydrology Model with the Penn State-NCAR MM5 Modeling System. Part I: Model Implementation and Sensitivity. *Mon. Weather Rev.* 129: 569–585.

Chou, M.D., Suarez, M.J., Ho, C.H., Yan, M.M.H. and Lee, K.T. (1998). Parameterizations for Cloud Overlapping and Shortwave Single-scattering Properties for Use in General Circulation and Cloud Ensemble Models. *J. Clim.* 11: 202–214, doi: 10.1175/1520-0442(1998)011<0202:PFCOAS>2.0.CO;2.

Crumeyrolle, S., Schwarzenboeck, A., Roger, J.C., Sellegri, K., Burkhart, J.F., Stohl, A., Gomes, L., Quennehen, B., Roberts, G., Weigel, R., Villani, P., Pichon, J M., Bourrianne, T. and Laj, P. (2013). Overview of Aerosol Properties Associated with Air Masses Sampled by the ATR-42 during the EUCAARI Campaign (2008). *Atmos. Chem. Phys.* 13: 4877–4893, doi: 10.5194/acp-13-4877-2013.

Dee, D.P., Uppala, S.M., Simmons, A.J., Berrisford, P., Poli, P., Kobayashi, S., Andrae, U., Balmaseda, M.A., Balsamo, G., Bauer, P., Bechtold, P., Beljaars, A.C.M., van de Berg, L., Bidlot, J., Bormann, N., Delsol, C., Dragani, R., Fuentes, M., Geer, A.J., Haimberger, L., Healy, S.B., Hersbach, H., Hólm, E.V., Isaksen, L., Kållberg, P., Köhler, M., Matricardi, M., McNally, A.P., Monge-Sanz, B.M., Morcrette, J.J., Park, B.K., Peubey, C., de Rosnay, P., Tavolato, C., Thépaut, J.N. and Vitart, F. (2011). The ERA-Interim Reanalysis: Configuration and Performance of the Data Assimilation System. *Q. J. R. Meteorolog. Soc.* 137: 553–597, doi: 10.1002/qj.828.

Donahue, N.M., Robinson, A.L., Stanier, C.O. and Pandis, S.N. (2006). Coupled Partitioning, Dilution, and Chemical Aging of Semivolatile Organics. *Environ. Sci. Technol.* 40: 2635–2643, doi: 10.1021/es052297c.

Emmons, L.K., Walters, S., Hess, P.G., Lamarque, J.F., Pfister, G.G., Fillmore, D., Granier, C., Guenther, A., Kinnison, D., Laepple, T., Orlando, J., Tie, X., Tyndall, G., Wiedinmyer, C., Baughcum, S.L. and Kloster, S. (2010). Description and Evaluation of the Model for Ozone and Related Chemical Tracers, Version 4 (MOZART-4). *Geosci. Model Dev.* 3: 43–67, doi: 10.5194/gmd-3-43-2010.

Fountoukis, C., Megaritis, A.G., Skyllakou, K., Charalampidis, P.E., Pilinis, C., Denier van der Gon, H. A.C., Crippa, M., Canonaco, F., Mohr, C., Prévôt, A.S. H., Allan, J.D., Poulain, L., Petäjä, T., Tiitta, P., Carbone, S., Kiendler-Scharr, A., Nemitz, E., O'Dowd, C., Swietlicki, E. and Pandis, S.N. (2014). Organic Aerosol Concentration and Composition over Europe: Insights from Comparison of Regional Model Predictions with Aerosol Mass Spectrometer Factor Analysis. *Atmos. Chem. Phys.* 14: 9061–9076, doi: 10.5194/acp-14-9061-2014.

Freney, E.J., Sellegri, K., Canonaco, F., Boulon, J., Hervo, M., Weigel, R., Pichon, J.M., Colomb, A., Prévôt, A.S.H. and Laj, P. (2011). Seasonal Variations in Aerosol Particle Composition at the Puy-de-Dôme Research Station in France. *Atmos. Chem. Phys.* 11: 13047–13059, doi: 10.5194/acp-11-13047-2011.

Freutel, F., Schneider, J., Drewnick, F., Weiden-Reinmüller, S.L. von der, Crippa, M., Prévôt, A.S.H., Baltensperger, U., Poulain, L., Wiedensohler, A., Sciare, J., Sarda-Estève, R., Burkhart, J.F., Eckhardt, S., Stohl, A., Gros, V., Colomb, A., Michoud, V., Doussin, J.F., Borbon, A., Haeffelin, M., Morille, Y., Beekmann, M. and Borrmann, S. (2013). Aerosol Particle Measurements at Three Stationary Sites in the Megacity of Paris during Summer 2009: Meteorology and Air Mass Origin Dominate Aerosol Particle Composition and Size Distribution. *Atmos. Chem. Phys.* 13: 933–959, doi: 10.5194/acp-13-933-2013.

Geiger, H., Barnes, I., Bejan, I., Benter, T. and Spittler, M. (2003). The Tropospheric Degradation of Isoprene: An Updated Module for the Regional Atmospheric Chemistry Mechanism. *Atmos. Environ.* 37: 1503–1519, doi: 10.1016/S1352-2310(02)01047-6.

Gelencsér, A., May, B., Simpson, D., Sánchez-Ochoa, A., Kasper-Giebl, A., Puxbaum, H., Caseiro, A., Pio, C. and Legrand, M. (2007). Source Apportionment of $PM_{2.5}$ Organic Aerosol over Europe: Primary/Secondary, Natural/Anthropogenic, and Fossil/Biogenic Origin. *J. Geophys. Res.* 112: D23S04, doi: 10.1029/2006JD008094.

Granier, C., Bessagnet, B., Bond, T., D'Angiola, A., Denier van der Gon, H., Frost, G., Heil, A., Kaiser, J., Kinne, S., Klimont, Z., Kloster, S., Lamarque, J.F., Liousse, C., Masui, T., Meleux, F., Mieville, A., Ohara, T., Raut, J.C., Riahi, K., Schultz, M., Smith, S., Thompson, A., van Aardenne, J., van der Werf, G. and van Vuuren, D. (2011). Evolution of Anthropogenic and Biomass Burning Emissions of Air Pollutants at Global and Regional Scales during the 1980–2010 Period. *Clim. Change* 109: 163–190, doi: 10.1007/s10584-011-0154-1.

Grell, G.A. and Dévényi, D. (2002). A Generalized Approach to Parameterizing Convection Combining Ensemble and Data Assimilation Techniques. *Geophys. Res. Lett.* 29: 38.1–38.4, doi: 10.1029/2002GL015311.

Grell, G.A., Peckham, S.E., Schmitz, R., McKeen, S.A., Frost, G., Skamarock, W.C. and Eder, B. (2005). Fully Coupled "Online" Chemistry within the WRF Model, *Atmos. Environ.*, 39: 6957–6975, doi: 10.1016/j.atmosenv.2005.04.027.

Guenther, A., Karl, T., Harley, P., Wiedinmyer, C., Palmer, P.I. and Geron, C. (2006). Estimates of Global Terrestrial Isoprene Emissions Using MEGAN (Model of Emissions of Gases and Aerosols from Nature). *Atmos. Chem. Phys.* 6: 3181–3210, doi: 10.5194/acp-6-3181-2006.

Hallquist, M., Wenger, J.C., Baltensperger, U., Rudich, Y., Simpson, D., Claeys, M., Dommen, J., Donahue, N. M., George, C. and Goldstein, A.H. (2009). The Formation, Properties and Impact of Secondary Organic Aerosol: Current and Emerging Issues. *Atmos. Chem. Phys.* 9: 5155–5236.

Hao, L.Q., Romakkaniemi, S., Yli-Pirilä, P., Joutsensaari, J., Kortelainen, A., Kroll, J.H., Miettinen, P., Vaattovaara, P., Tiitta, P., Jaatinen, A., Kajos, M. K., Holopainen, J. K., Heijari, J., Rinne, J., Kulmala, M., Worsnop, D.R., Smith, J.N. and Laaksonen, A. (2011). Mass Yields of Secondary Organic Aerosols from the Oxidation of α-pinene and Real Plant Emissions. *Atmos. Chem. Phys.* 11: 1367–1378, doi: 10.5194/acp-11-1367-2011.

Hervo, M., Sellegri, K., Pichon, J.M., Roger, J.C. and Laj, P.

(2014). Long Term Measurements of Optical Properties and Their Hygroscopic Enhancement. *Atmos. Chem. Phys. Discuss.* 14: 27731–27767, doi: 10.5194/acpd-14-27731-2014.

Hong, S.Y., Noh, Y. and Dudhia, J. (2006). A New Vertical Diffusion Package with an Explicit Treatment of Entrainment Processes. *Mon. Weather Rev.* 134: 2318–2341, doi: 10.1175/MWR3199.1.

IPCC (2013). Climate Change 2013 : The Physical Science Basis.

Kiendler-Scharr, A., Mensah, A.A., Friese, E., Topping, D., Nemitz, E., Prevot, A.S.H., Äijälä, M., Allan, J., Canonaco, F., Canagaratna, M., Carbone, S., Crippa, M., Dall Osto, M., Day, D.A., De Carlo, P., Di Marco, C.F., Elbern, H., Eriksson, A., Freney, E., Hao, L., Herrmann, H., Hildebrandt, L., Hillamo, R., Jimenez, J.L., Laaksonen, A., McFiggans, G., Mohr, C., O'Dowd, C., Otjes, R., Ovadnevaite, J., Pandis, S.N., Poulain, L., Schlag, P., Sellegri, K., Swietlicki, E., Tiitta, P., Vermeulen, A., Wahner, A., Worsnop, D. and Wu, H.C. (2015). Organic Nitrates from Night-time Chemistry are Ubiquitous in the European Submicron Aerosol. *Nature*, Submitted.

Knote, C., Brunner, D., Vogel, H., Allan, J., Asmi, A., Äijälä, M., Carbone, S., van der Gon, H. D., Jimenez, J. L., Kiendler-Scharr, A., Mohr, C., Poulain, L., Prévôt, A. S.H., Swietlicki, E. and Vogel, B. (2011). Towards an Online-coupled Chemistry-climate Model: Evaluation of Trace Gases and Aerosols in COSMO-ART. *Geosci. Model Dev.* 4: 1077–1102, doi: 10.5194/gmd-4-1077-2011.

Langmann, B., Sellegri, K. and Freney, E. (2014). Secondary Organic Aerosol Formation during June 2010 in Central Europe: Measurements and Modelling Studies with a Mixed Thermodynamic-kinetic Approach. *Atmos. Chem. Phys.* 14: 3831–3842, doi: 10.5194/acp-14-3831-2014.

Lanz, V.A., Prévôt, A.S.H., Alfarra, M.R., Weimer, S., Mohr, C., DeCarlo, P.F., Gianini, M.F.D., Hueglin, C., Schneider, J., Favez, O., D'Anna, B., George, C. and Baltensperger, U. (2010). Characterization of Aerosol Chemical Composition with Aerosol Mass Spectrometry in Central Europe: An Overview. *Atmos. Chem. Phys.* 10: 10453–10471, doi: 10.5194/acp-10-10453-2010.

Middleton, P., Stockwell, W.R. and Carter, W.P. (1990). Aggregation and Analysis of Volatile Organic Compound Emissions for Regional Modeling. *Atmos. Environ.* 24: 1107–1133.

Mlawer, E.J., Taubman, S.J., Brown, P.D., Iacono, M.J. and Clough, S.A. (1997). Radiative Transfer for Inhomogeneous Atmospheres: RRTM, a Validated Correlated-k Model for the Longwave. *J. Geophys. Res.* 102: 16663–16682, doi: 10.1029/97JD00237.

Morrison, H., Thompson, G. and Tatarskii, V. (2009). Impact of Cloud Microphysics on the Development of Trailing Stratiform Precipitation in a Simulated Squall Line: Comparison of One- and Two-moment Schemes. *Mon. Weather Rev.* 137: 991–1007, doi: 10.1175/2008 MWR2556.1.

Murphy, B.N. and Pandis, S.N. (2009). Simulating the Formation of Semivolatile Primary and Secondary Organic Aerosol in a Regional Chemical Transport Model. *Environ. Sci. Technol.* 43: 4722–4728, doi: 10.1021/es803168a.

Shrivastava, M., Fast, J., Easter, R., Gustafson Jr., W., Zaveri, R.A., Jimenez, J.L., Saide, P. and Hodzic, A. (2011). Modeling Organic Aerosols in a Megacity: Comparison of Simple and Complex Representations of the Volatility Basis Set Approach. *Atmos. Chem. Phys.* 11: 6639–6662, doi: 10.5194/acp-11-6639-2011.

Stockwell, W.R., Kirchner, F., Kuhn, M. and Seefeld, S. (1997). A New Mechanism for Regional Atmospheric Chemistry Modeling. *J. Geophys. Res.* 102: 25847–25879, doi: 199710.1029/97JD00849.

Tsimpidi, A.P., Karydis, V.A., Zavala, M., Lei, W., Molina, L., Ulbrich, I.M., Jimenez, J.L. and Pandis, S.N. (2010). Evaluation of the Volatility Basis-set Approach for the Simulation of Organic Aerosol Formation in the Mexico City Metropolitan Area. *Atmos. Chem. Phys.* 10: 525–546, doi: 10.5194/acp-10-525-2010.

Wiedinmyer, C., Akagi, S.K., Yokelson, R.J., Emmons, L.K., Al-Saadi, J.A., Orlando, J.J. and Soja, A.J. (2011). The Fire INventory from NCAR (FINN): A High Resolution Global Model to Estimate the Emissions from Open Burning. *Geosci. Model Dev.* 4: 625–641, doi: 10.5194/gmd-4-625-2011.

Zhang, Q., Jimenez, J.L., Canagaratna, M.R., Allan, J.D., Coe, H., Ulbrich, I., Alfarra, M.R., Takami, A., Middlebrook, A.M. and Sun, Y.L. (2007). Ubiquity and Dominance of Oxygenated Species in Organic Aerosols in Anthropogenically-influenced Northern Hemisphere Midlatitudes. *Geophys. Res. Lett.* 34: L13801.

Zhang, Q., Jimenez, J.L., Canagaratna, M.R., Ulbrich, I.M., Ng, N.L., Worsnop, D.R. and Sun, Y. (2011). Understanding Atmospheric Organic Aerosols via Factor Analysis of Aerosol Mass Spectrometry: A Review. *Anal. Bioanal. Chem.* 401: 3045–3067, doi: 10.1007/s00216-011-5355-y.

Zhang, Q.J., Beekmann, M., Drewnick, F., Freutel, F., Schneider, J., Crippa, M., Prevot, A.S.H., Baltensperger, U., Poulain, L., Wiedensohler, A., Sciare, J., Gros, V., Borbon, A., Colomb, A., Michoud, V., Doussin, J.F., Denier van der Gon, H.A.C., Haeffelin, M., Dupont, J.C., Siour, G., Petetin, H., Bessagnet, B., Pandis, S.N., Hodzic, A., Sanchez, O., Honoré, C. and Perrussel, O. (2013). Formation of Organic Aerosol in the Paris Region during the MEGAPOLI Summer Campaign: Evaluation of the Volatility-basis-set Approach within the CHIMERE Model. *Atmos. Chem. Phys.* 13: 5767–5790, doi: 10.5194/acp-13-5767-2013.

Zhang, X., Cappa, C.D., Jathar, S.H., McVay, R.C., Ensberg, J.J., Kleeman, M.J. and Seinfeld, J.H. (2014). Influence of Vapor Wall Loss in Laboratory Chambers on Yields of Secondary Organic Aerosol. *Proc. Natl. Acad. Sci. U.S.A.* 111: 5802–5807, doi: 10.1073/pnas.1404727111.

Received for review, May 15, 2015
Revised, September 25, 2015
Accepted, November 5, 2015